

ANALYTICAL STUDY OF EFFECT OF ENERGY BAND PARAMETERS AND LATTICE TEMPERATURE ON CONDUCTION BAND OFFSET IN AlN/Ga₂O₃ HEMT *

Rajan Singh¹, Trupti Ranjan Lenka¹, Hieu Pham Trung Nguyen²

¹Department of Electronics and Communication Engineering,
National Institute of Technology Silchar, Assam, India

²Department of Electrical and Computer Engineering, New Jersey Institute of Technology,
Newark, New Jersey, 07102, USA

Abstract. *Apart from other factors, band alignment led conduction band offset (CBO) largely affects the two dimensional electron gas (2DEG) density n_s in wide bandgap semiconductor based high electron mobility transistors (HEMTs). In the context of assessing various performance metrics of HEMTs, rational estimation of CBO and maximum achievable 2DEG density is critical. Here, we present an analytical study on the effect of different energy band parameters—energy bandgap and electron affinity of heterostructure constituents, and lattice temperature on CBO and estimated 2DEG density in quantum triangular-well. It is found that at thermal equilibrium, n_s increases linearly with ΔEC at a fixed Schottky barrier potential, but decreases linearly with increasing gate-metal work function even at fixed ΔEC , due to increased Schottky barrier heights. Furthermore, it is also observed that poor thermal conductivity led to higher lattice temperature which results in lower energy bandgap, and hence affects ΔEC and n_s at higher output currents.*

Key words: *2DEG density, CBO Conduction Band Offset, Heterojunction, HEMT, Lattice Temperature, Barrier, Buffer, Ga₂O₃*

1. INTRODUCTION

Due to its suitable material properties and availability of high quality and cost-effective native substrates, gallium oxide (Ga₂O₃) is being exhaustively investigated for power electronics applications [1]. Currently, this domain of high-power and high-frequency devices are dominated by wide-bandgap semiconductors like silicon carbide (SiC) and gallium nitride (GaN). Some of the unique features—excellent carrier confinement in the form of 2DEG, high

Received February 10, 2021; received in revised form May 06, 2021

Corresponding author: Rajan Singh

Department of Electronics and Communication Engineering, National Institute of Technology Silchar, Assam, India

E-mail: rajan_rs@ece.nits.ac.in

* An earlier version of this paper was presented at the International Conference on Micro/Nanoelectronics Devices, Circuits, and Systems (MNDCS-2021), January 29-31, 2021, India [1].

carrier mobility, and large breakdown voltage of GaN-based HEMTs have made it one of the most useful devices for high-power and high-frequency applications [2-4]. Despite some key challenges on the substrate side, GaN technology however survived beyond the expected life cycle of a typical semiconductor technology [5]. Recently, researchers across the globe have started to look towards ultra-wide bandgap (UWB) semiconductors—Ga₂O₃, AlN, and Diamond for high voltage applications [6]. Among these UWB semiconductors, Ga₂O₃ has emerged as an ultimate choice for future power electronics devices on the back of preliminary results that are encouraging enough to prove its capabilities to supplement existing SiC/GaN technologies. It is worth noting here that, apart from lower bulk electron mobility, 150 - 200 cm²/Vs [5-6], Ga₂O₃ has very low thermal conductivity, 0.13 – 0.27 W/cm K [5]. The following equation relates the electron affinity of a semiconductor with lattice temperature (T_L), as given in [7]:

$$\chi(T_L) = \chi(300) - CHI.EG.TDEP \times (E_g(T_L) - E_g(300)) \quad (1)$$

where, parameter *CHIEG.TDEP* is a ratio, in range (0 – 1) with a default value of 0.5 (used here), which specifies a fraction of the change in the bandgap due to the temperature change. For β -Ga₂O₃, the energy bandgap at T_L is given by Varshni equation [8]:

$$E_g(T_L) = E_g(300) - \frac{\alpha T_L^2}{T_L + \beta} \quad (2)$$

where fitting parameters α , and β for AlN, and β -Ga₂O₃ are taken from [9], [10] respectively and extrapolated at higher temperatures.

The different bandgaps of two materials of heterojunction create these band discontinuities, and the band offset parameters—conduction and valence band offset (ΔE_C and ΔE_V) have a large impact on the charge transport in the heterostructure [7]. Higher values of 2DEG density are anticipated for large ΔE_C values [11], while ΔE_C is also dependent on different electron affinity values of heterojunction materials besides their bandgaps as stated earlier. Considering the importance of 2DEG density in the operation of HEMTs, various physics-based analytical models for n_s , [12-18] are available mostly for AlGaN/GaN HEMTs. In this work, we primarily investigated the estimation of n_s , based on different values of alignment—a fraction of bandgap difference to ΔE_C , at fixed Schottky barrier and at higher metal work function led increasing Schottky potential at fixed ΔE_C through TCAD simulations. The study is also done considering the heat flow in the device as the poor thermal conductivity of Ga₂O₃ and high currents in power devices resulting in high lattice temperature.

Table 1 Symbols Used and Meaning [1]

Symbol	Physical meaning	Symbol	Physical meaning
χ	Electron affinity	ϵ	Static dielectric permittivity
E_g	Energy bandgap	D	Density of states
ϕ_B	Schottky barrier height	E_f	Position of Fermi level
ϕ_M	Metal work function	d	Thickness of barrier layer
q	Electron charge	qV_0	Built-in potential
n_s	Electron density in the 2DEG	V_{th}	Thermal voltage
ΔE_C	Conduction band offset (CBO)	N_c	Conduction band density
ΔE_V	Valence band offset (VBO)	N_v	Valence band density

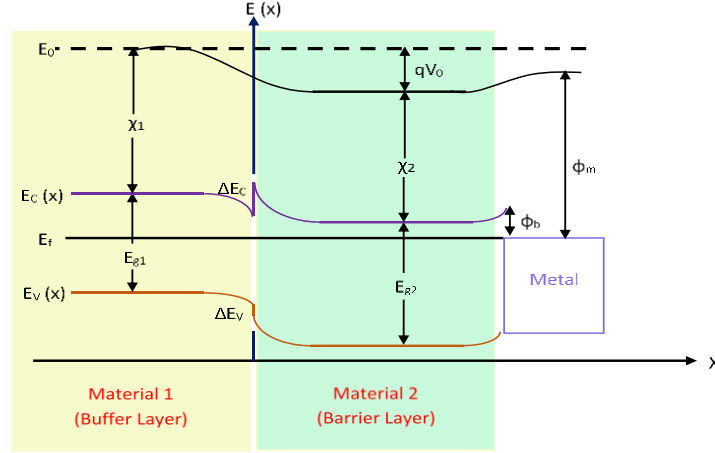


Fig. 1 Energy band diagram of a typical heterojunction showing band offset [1].

The energy band diagram of AlN/ β -Ga₂O₃ abrupt heterojunction, having β -Ga₂O₃ buffer layer (E_{g1} , and χ_1) and AlN barrier layer (E_{g2} , and χ_2), where $E_{g2} > E_{g1}$ and $\chi_2 < \chi_1$ is shown in Figure 1. The developed model is used to optimize n_s considering band parameters of barrier and buffer layer materials reported in Ga₂O₃ experimental HEMTs. The 2DEG charge density n_s relating conduction band offset ΔE_C , using charge control equation [12], can be written as:

$$n_s = \frac{\epsilon}{qa} [V_g - \phi_b + V_{pb} - E_f + \Delta E_C] \quad (3)$$

where V_{pb} is barrier layer pinch-off voltage and V_g is the applied gate voltage. The other symbols used along with their physical meaning are listed in Table 1. The device under study here is AlN/ β -Ga₂O₃ HEMTs, as the experimental measurements of band offset parameters— ΔE_V and ΔE_C at the III-nitride (GaN, and AlN)/ β -Ga₂O₃ heterostructure are readily available [19, 20]. Additionally, as the in-plane lattice mismatch between [-201] AlN and [0002] AlN planes is as small as 2.4 % [20], AlN/ β -Ga₂O₃ is anticipated as a potential candidate for future high-power applications.

2. 2DEG CHARGE DENSITY AND DEVICE MODEL DESCRIPTION

In the triangular quantum well, 2DEG charge density n_s is related with Fermi level E_f and two sub-bands E_0 and E_1 , using Fermi-Dirac statistics, as given by [12]

$$n_s = DV_{th} \left[\ln \left\{ e^{(E_f - E_0)/V_{th}} + 1 \right\} + \ln \left\{ e^{(E_f - E_1)/V_{th}} + 1 \right\} \right] \quad (4)$$

where first energy level $E_0 = \gamma_0 n_s^{2/3}$, and second $E_1 = \gamma_1 n_s^{2/3}$. In case of complete ionization of barrier layer, equation (1) can be written as:

$$n_s = \frac{\epsilon}{qa} \{V_{go} - E_f\} \quad (5)$$

where $V_{go} = V_g - V_{off}$. The 2DEG density model, for AlGaIn/GaN HEMT, developed so far explained n_s behavior concerning V_g . It was assumed that only the first sub-band E_0 lies

below E_f for $V_g > V_{off}$. Here, a more simplified expression of Fermi level (in volts) in terms of n_s is obtained under steady-state conditions.

$$E_f = \frac{n_s}{2D} + \frac{E_0 + E_1}{2} - \frac{V_{th}}{2} \quad (6)$$

The above equation is obtained using the approximation $\ln(1+x) \approx x$, for $x \ll 1$ and after some mathematical manipulations. Next, E_0 and E_1 can be replaced to get the following explicit relation between E_f and n_s :

$$E_f = \frac{n_s}{2D} + \left(\frac{\gamma_0 + \gamma_1}{2}\right) n_s^{2/3} - \frac{V_{th}}{2} \quad (7)$$

Furthermore, higher charge confinement in the triangular well is anticipated based on higher energy difference between E_f and E_0 [21]. It is worth mentioning that, some fraction, say 60 or 80 % and very rarely up to 100% [22], of the heterostructures' material bandgap difference appears as CBO. Therefore, while estimating n_s , careful measurement of CBO (ΔE_C) is important. In this work, for the estimation of confined charge density in the quantum well, the relative position of E_0 to E_f is analyzed under varying band alignment and varying Schottky barrier height under thermal equilibrium. This is illustrated in Figure 2.

The device model analyzed here is comprised of an AlN barrier on β -Ga₂O₃ buffer layer having a thickness of 10 and 50 nm respectively. The layer sequence cum device cross-section is shown in Figure 3. Source and drain contacts are considered to be ohmic, while gate contact is Schottky type. Silicon nitride (Si₃N₄) is used for surface passivation and to limit the parasitic capacitances as mentioned in [23]. The various material parameters for β -Ga₂O₃ are taken from [24, 25] and are shown in Table 2 along with for AlN taken from [7]. Different material parameters used in the simulation of AlN/ β -Ga₂O₃ HEMT constituents are listed in Table 2.

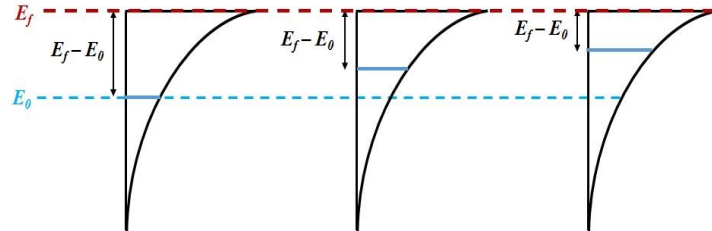


Fig. 2 The relative position of E_0 and E_f to CBO for fixed Schottky potential [1].

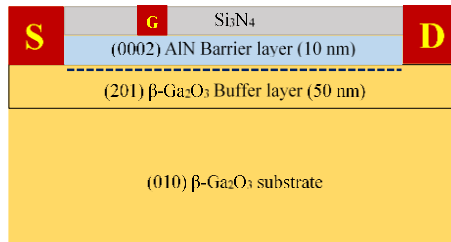


Fig. 3 Schematic diagram showing layer sequence of AlN/ β -Ga₂O₃ HEMT; dashed line below AlN barrier represents 2DEG charges [1].

Table 2 Material parameters of β -Ga₂O₃ and AlN used in different calculations of TCAD simulations, taken from [7, 24-25].

Symbol	β -Ga ₂ O ₃	AlN
χ (eV)	3.15	1.4
E_g (eV)	4.9	6.1
N_c (cm ⁻³)	3.6×10^{18}	4.42×10^{18}
N_v (cm ⁻³)	2.86×10^{20}	6.76×10^{18}
n_i (cm ⁻³)	2.23×10^{-22}	1.51×10^{-33}
ϵ	10.2	8.5

3. RESULTS AND DISCUSSION

The device under the test (Figure 3) is simulated to estimate CBO and 2DEG density using Atlas TCAD under steady-state conditions and at different bias voltages enabling heat-flow in the device. The duo investigations are performed using the alignment-based rule— ΔE_C as a fraction of ΔE_g , due to the significant difference between band offsets estimated using standard values of electron affinity and experimental measurements.

3.1. At Steady State Condition

3.1.1. Fixed Schottky Barrier Height

Earlier, various high-performance AlN Schottky barrier diodes were demonstrated [26-28] and barrier heights ranging from 1.6 – 2.3 eV between AlN and different metals were measured [26]. Here, Ti and Au AlN Schottky contacts with a barrier height of 1.6 eV are used to estimate CBO and analyze 2DEG density under three different degrees of alignments—60, 80, and 100%. As conduction band offset ΔE_C increased from 0.65 to 1.15 eV, 2DEG density increases as higher conduction band alignment boost carrier confinement as illustrated in Figure 4.

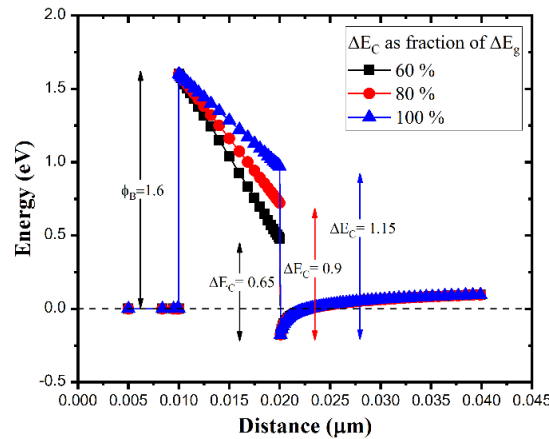


Fig. 4 Estimation of CBO keeping fixed barrier height of 1.6 eV under 60, 80, and 100% alignment of bandgap difference.

3.1.2. Fixed alignment of 60%

Considering a moderate value of alignment, say 60% of the bandgap difference ($\Delta E_g = 1.24$ eV) between AlN and β -Ga₂O₃ is assigned here as CBO. The three different metals—Ti, Ni, and Au on AlN with barrier heights of 1.6, 1.8, and 2.3 eV are considered to analyze to estimate ΔE_C and consequently 2DEG density and are shown in Figure 5. Although, a fixed fraction of bandgap difference (0.6 of 1.24 = 0.744 eV) is assigned to conduction band discontinuity, the estimated value of ΔE_C is slightly less than the assigned value. This may be attributed to surface and or interface states at the AlN/ β -Ga₂O₃ boundary [26].

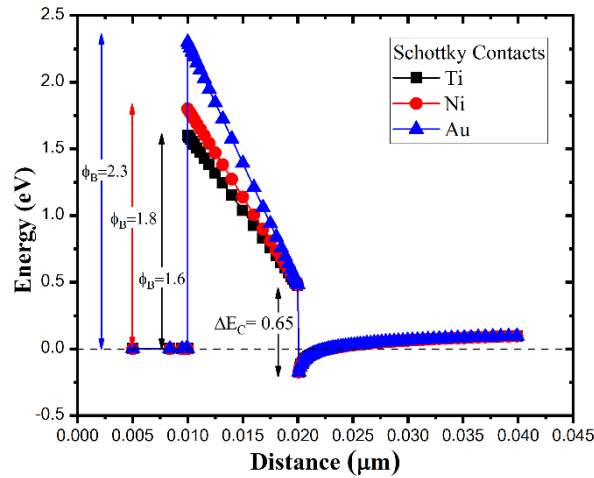


Fig. 5 Estimation of ΔE_C , and n_s under three increasing Schottky barrier heights for fixed alignment of 60 %; decreasing values of n_s ($5.0, 4.9,$ and 4.7) $\times 10^{13}$ cm^{-2} are estimated.

3.2. Heat-flow Simulation

Poor thermal conductivity of Ga₂O₃ and higher output currents in Ga₂O₃ based power devices commonly result in high lattice temperature in absence of device-level thermal management. Here, after enabling the relevant model in simulation, maximum lattice temperature under the gate area is gauged under different bias voltages. The subsequent effects on electron affinity and energy bandgap are also estimated. The increased affinity values led to reduced energy bandgap results in higher bandgap difference at the heterointerface. The maximum lattice temperature at elevated currents is shown in Figure 6, and resulting energy bandgap and electron affinity at different lattice temperature is shown in Figure 7.

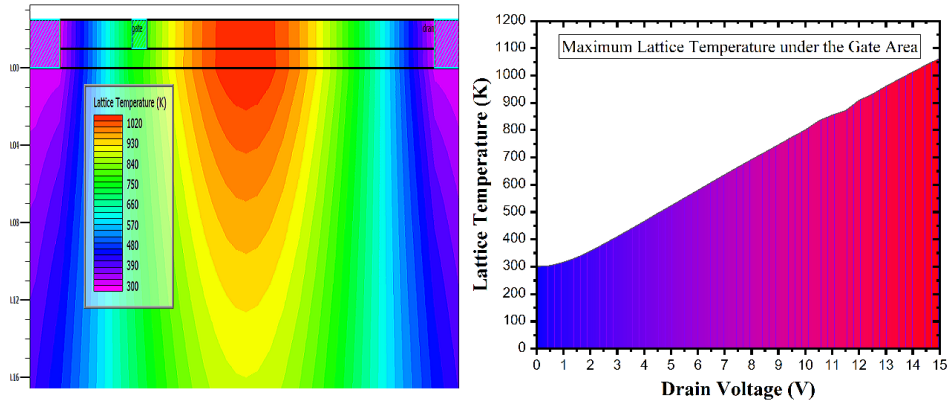


Fig. 6 Maximum lattice temperature; extracted from ATLAS (left) at higher drain current, and plotted versus corresponding drain voltage at zero gate voltage (right).

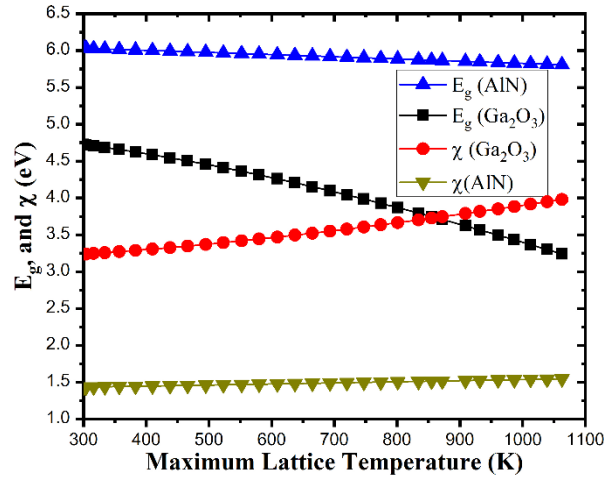


Fig. 7 Energy band gap and electron affinity as a function of maximum lattice temperature.

3.2.1. Effect on Conduction band offset

As the lattice temperature increases, the energy bandgap of β -Ga₂O₃ shrinks as per equation (2) and is shown in Figure 7. Now the maximum bandgap difference available between AlN and β -Ga₂O₃, corresponding to the maximum lattice temperature of 1063 K at V_{DS} = 15 V (V_{GS} = 0 V), is given as

$$\Delta E_g = (E_g^{AlN} - E_g^{Ga_2O_3}) \approx 5.8 - 3.2 \approx 2.6 \text{ eV}$$

Here, it is evident that a larger change in Ga₂O₃ energy bandgap led to a 46 % higher bandgap difference between AlN and Ga₂O₃ compared to its value, 1.24 eV, at 300 K and consequently higher values of CBO result. Further, corresponding to 80 % alignment of

ΔE_g ($\Delta E_C = 0.8 \times 2.6 = 2.08$ eV), 2DEG density n_s is estimated for trio barrier heights and is shown in Figure 8.

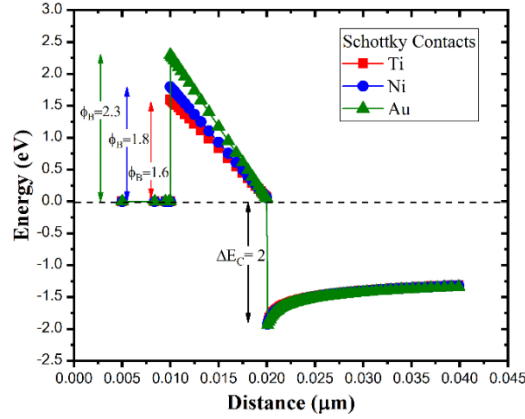


Fig. 8 2DEG estimation at the fixed alignment of 80 % for different Schottky barrier heights. 2DEG density decreases with higher Schottky barrier heights.

The important inferences from the results exhibited above are summarized in Table 3. It is found that a higher degree of CBO results in increased 2DEG density, both at steady-state and at higher bias voltages. However, 2DEG density in the latter scenario is relatively low as compared to the previous case. This is attributed to the enhanced electron-phonon interaction with increasing lattice temperature. Additionally, confined carrier density decreases with increasing Schottky barrier heights in both cases. This can be due to the presence of interface charges and defect states at the AlN- β -Ga₂O₃ boundary.

Table 3 Estimated values of ΔE_C , and n_s under fixed Schottky barrier and fixed alignment

Alignment (%) / Schottky height (eV)	Under steady state ($T_L = 300$ K)		At $V_{DS}/V_{GS} = 15 / 0V$ ($T_L = 1063$ K)	
	$E_g^{\beta-Ga_2O_3} = 4.9$ eV, $E_g^{AlN} = 6.1$ eV		$E_g^{\beta-Ga_2O_3} = 3.2$ eV, $E_g^{AlN} = 5.8$ eV	
	ΔE_C (eV)	$n_s (\times 10^{13} \text{ cm}^{-2})$	ΔE_C (eV)	$n_s (\times 10^{13} \text{ cm}^{-2})$
60 / 1.6	0.65	5.0	1.47	4.6
80 / 1.6	0.9	5.12	2.0	4.8
100 / 1.6	1.15	5.23	2.5	5.0
80 / 1.6	0.9	5.12	2.0	4.8
80 / 1.8	0.9	5.0	2.0	4.7
80 / 2.3	0.9	4.8	2.0	4.5

4. CONCLUSION

To summarize, the effect of energy bandgap difference enabled conduction band offset on 2DEG density in AlN/ β -Ga₂O₃ HEMT is studied analytically. The analytical expression of Fermi level is derived to conclude that the relative position of E_f and E_0 largely affects 2DEG density. Alignment-based rule—CBO as a fraction of ΔE_g is found in more agreement with its value measured in experimental devices. By varying band alignment

and Schottky barrier heights, the resultant effect on ΔE_C and 2DEG density are estimated. It is found that apart from conduction band offset dependency, n_s is also affected by Schottky barrier height. It is also shown that poor thermal conductivity led to higher lattice temperature which results in large ΔE_g and CBO, but yielded relatively lower 2DEG density as compared to steady-state condition. In steady-state, for fixed Schottky barrier height of $\phi_B = 1.6$ eV (Ti/AlN), 2DEG density increases from 5.0×10^{13} to 5.23×10^{13} cm⁻² when ΔE_C changes from 60 to 100 %, and from 4.6×10^{13} to 5.0×10^{13} cm⁻² at $V_{DS}/V_{GS} = 15/0$ V. On the other hand, even at fixed ΔE_C , 2DEG density decreases from 5.12×10^{13} to 4.8×10^{13} cm⁻² when ϕ_B increases from 1.6 to 2.3 eV in steady-state, and 4.8×10^{13} to 4.5×10^{13} cm⁻² at lattice temperature of 1063 K corresponding to $V_{DS}/V_{GS} = 15/0$ V. These conclusions can be beneficial to access the limitations in β -Ga₂O₃ HEMT performance, which critically depends on the careful estimation of 2DEG density.

REFERENCES

- [1] R. Singh, T. R. Lenka, S. A. Ahsan, and H. P. T. Nguyen, "Analytical Study of Conduction Band Discontinuity supported 2DEG Density in AlN/Ga₂O₃ HEMT," In Proceedings of the International Conference on Micro/Nanoelectronics Devices, Circuits, and Systems (MNDCS-2021), 29-31 Jan 2021. <http://mndcs.nits.ac.in/>
- [2] U. K. Mishra, L. Shen, T. E. Kazior, Y. F. Wu, "GaN-based RF power devices and amplifiers," In Proceedings of the IEEE, 16, Jan 2008, vol. 96, no. 2, pp. 287–305.
- [3] P. Parikh, Y. Wu, M. Moore, P. Chavarkar, U. Mishra, R. Neidhard, et al., "High linearity, robust, AlGaIn-GaN HEMTs for LNA and receiver ICs," In Proceedings of the IEEE Lester Eastman Conf. High Perform. Devices, Aug. 2002, pp. 415–421.
- [4] P. Kordos, A. Alam, J. Betko, P. P. Chow, M. Heuken, P. Javorka, et al., "Material and device issues of GaN-based HEMTs," In Proceedings of the 8th IEEE Int. Symp. High Perform. Electron Devices Microw. Optoelectron. Appl., Nov. 2002, pp. 61–66.
- [5] S. J. Pearton, F. Ren, M. Tadjer, and J. Kim, "Perspective: Ga₂O₃ for ultra-high power rectifiers and MOSFETs," *Journal of Applied Physics*, vol. 124, no. 22, p. 220901, Dec 2018.
- [6] E. Ahmadi, and Y. Oshima, "Materials issues and devices of α - and β -Ga₂O₃," *Journal of Applied Physics*, vol. 126, p. 160901, Oct. 2019.
- [7] Atlas, Device Simulator. "Atlas user's manual." Silvaco International Software, Santa Clara, CA, USA (2016).
- [8] Y. P. Varshni, "Temperature dependence of the energy gap in semiconductors," *Physica* 34, vol. 1, pp. 149–154, 1967.
- [9] S. Rafique, L. Han, S. Mou, and H. Zhao, "Temperature and doping concentration dependence of the energy band gap in β -Ga₂O₃ thin films grown on sapphire," *Optical Material Express* 3561, vol. 7, no. 10, Oct. 2017.
- [10] K. B. Nam, J. Li, J. Y. Lin, and H. X. Jiang, "Optical properties of AlN and GaN in elevated temperatures," *Applied Physics Letters*, vol. 85, no. 16, Oct 2004.
- [11] Y. Zhang, et al., "Demonstration of high mobility and quantum transport in modulation-doped β -(Al_xGa_{1-x})₂O₃/Ga₂O₃ heterostructures," *Applied Physics Letters*, vol. 112, no. 17, p. 173502, Apr. 2018.
- [12] S. Kola, J. M. Golio, and G. N. Maracas, "An analytical expression for Fermi level versus sheet carrier concentration for HEMT modeling," *IEEE Electron Device Lett.*, vol. 9, no. 3, pp. 136–138, Mar. 1988.
- [13] X. Cheng, M. Li, and Y. Wang, "An analytical model for current voltage characteristics of AlGaIn/GaN HEMTs in presence of self-heating effect," *Solid State Electron.*, vol. 54, no. 1, pp. 42–47, Jan. 2010.
- [14] S. Khandelwal, N. Goyal, and T. A. Fjeldly, "A physics based analytical model for 2DEG charge density in AlGaIn/GaN HEMT devices," *IEEE Trans. Electron Devices*, vol. 58, no. 10, pp. 3622–3625, Oct. 2011.
- [15] X. Cheng and Y. Wang, "A surface-potential-based compact model for AlGaIn/GaN MODFETs," *IEEE Trans. Electron Devices*, vol. 58, no. 2, pp. 448–454, Feb. 2011.
- [16] T. R. Lenka, and A. K. Panda, "Effect of structural parameters on 2DEG density and $C \sim V$ characteristics of Al_xGa_{1-x}N/AlN/GaN-based HEMT," *Indian Journal of Pure & Applied Physics*, vol. 49, pp. 416–422, Jun 2011.
- [17] S. Khandelwal and T. A. Fjeldly, "A physics based compact model for I–V and C–V characteristics in AlGaIn/GaN HEMT devices," *Solid State Electron.*, vol. 76, pp. 60–66, Oct. 2012.

- [18] F. M. Yigletu, S. Khandelwal, T. A. Fjeldly, and B. Iniguez, "Compact Charge-Based Physical Models for Current and Capacitances in AlGaIn/GaN HEMTs," *IEEE Trans. Electron Devices*, vol. 60, no. 11, pp. 3746–3752, Nov. 2013.
- [19] W. Wei, et al., "Valence band offset of β -Ga₂O₃/wurtzite GaN heterostructure measured by X-ray photoelectron spectroscopy," *Nanoscale Research Letters*; vol. 7, p. 562, Dec. 2012.
- [20] H. Sun, et al., "Valence and conduction band offsets of β -Ga₂O₃/AlN heterojunction," *Applied Physics Letters*, vol. 111, no. 16, p. 162105, Oct. 2017.
- [21] Y. K. Verma, V. Mishra, S. K. Gupta, "A Physics Based Analytical Model for MgZnO/ZnO HEMT," *Journal of Circuits, Systems, and Computers*, Jan 2019.
- [22] H. Sun et al., "Nearly-zero valence band and large conduction band offset at BAlN/GaN heterointerface for optical and power device application," *Applied Surface Science*, vol. 458, pp. 949–953, Jul. 2018.
- [23] R. Singh, T R Lenka, R T Velpula, B Jain, H Q T Bui, H P T Nguyen, "A novel β -Ga₂O₃ HEMT with f_T of 166 GHz and X-band P_{OUT} of 2.91 W/mm," *Int. J. Numer Model El.*, e2794, 2020.
- [24] A. Mock, R. Korlacki, C. Briley, V. Darakchieva, B. Monemar, Y. Kumagai, K. Goto, M. Higashiwaki, M. Schubert, *Phys. Rev. B Condens. Matter*, vol. 96, no. 24, p. 245205, 2017.
- [25] Z. Zhang, E. Farzana, A.R. Arehart, and S.A. Ringel, "Deep level defects throughout the bandgap of (010) β -Ga₂O₃ detected by optically and thermally stimulated defect spectroscopy," *Applied Physics Letters*, vol. 108, p. 052105, Feb. 2016.
- [26] P. Reddy, I. Bryan, Z. Bryan, J. Tweedie, R. Kirste, R. Collazo, and Z. Sitar, "Schottky contact formation on polar and nonpolar AlN," *Journal Applied Physics*, vol. 116, no. 19, p. 194503, Nov. 2014.
- [27] Y. Irokawa, E. Villora, and K. Shimamura, "Schottky Barrier Diodes on AlN Free-Standing Substrates," *Japanese Journal of Applied Physics*, vol. 51, no. 4R, p. 040206, Mar. 2012.
- [28] T. Kinoshita, T. Nagashima, T. Obata, S. Takashima, R. Yamamoto, R. Togashi, Y. Kumagai, R. Schlessler, R. Collazo, A. Koukitu, and Z. Sitar, "Fabrication of vertical Schottky barrier diodes on n-type freestanding AlN substrates grown by hydride vapor phase epitaxy," *Appl. Phys. Exp.*, vol. 8, no. 6, p. 061003, May 2015.